

## High-speed force sensor for force microscopy and profilometry utilizing a quartz tuning fork

Franz J. Giessibl<sup>a)</sup>

Universität Augsburg, Institute of Physics, and EKM, Experimentalphysik VI, 86135 Augsburg, Germany

(Received 31 August 1998; accepted for publication 21 October 1998)

Force sensors are key elements of atomic force microscopes and surface profilometers. Sensors with an integrated deflection meter are particularly desirable. Here, quartz tuning forks as used in watches are utilized as force sensors. A novel technique is employed which simplifies the interpretation of the data and increases the imaging speed by at least one order of magnitude compared to previous implementations. The variation of the imaging signal with distance fits well to a Hertzian contact model. Images of compact discs and calibration gratings, which have been obtained with scanning speeds up to 230  $\mu\text{m/s}$ , are presented. © 1998 American Institute of Physics. [S0003-6951(98)00152-1]

The heart of both atomic force microscopes<sup>1</sup> (AFM) and surface profilometers<sup>2</sup> is the force sensor with tip which maps the surface. The forces acting on the tip are usually sensed by mounting the tip on a cantilever beam (CL) and measuring its deflection. Optical detection is the most common method to detect the deflection of the CL,<sup>3</sup> but also integrated deflection sensors based on the piezoresistive<sup>4</sup> or piezoelectric<sup>5</sup> effect are available. Here, it is demonstrated that quartz tuning forks<sup>6</sup> which are produced by the millions annually mainly for frequency normals in the watch industry can be used as force sensors for AFMs or profilometers. Güethner *et al.*<sup>7</sup> have used tuning forks as a force sensor in acoustic near field microscopy and Karrai *et al.*<sup>8</sup> have used a tuning fork to control the distance between the optical fiber and the surface in a scanning near-field-optical microscope. Recently, Edwards *et al.*<sup>9</sup> have demonstrated a faster mode using a phase-locked-loop detector.

In all the applications above, the fork is mounted in a similar manner as in a watch: the base part is fixed and both prongs are oscillating opposed to each other. The dynamical forces of the two prongs are then compensated in the base part. Since the base part and prongs are made out of a single quartz crystal, internal dissipation is low in this oscillation mode and the  $Q$  value is extremely high (up to 100 000 in vacuum and 10 000 in air). However, the symmetry of the prongs is broken when one of them is subject to a tip-sample interaction. Even conservative tip-sample forces cause damping in this mode, only slow scanning speeds are possible and the imaging signal is very difficult to interpret. Fixing one of the prongs firmly to a supporting structure overcomes this problem (“ $q$ Plus-sensor”<sup>10</sup>) and allows using tuning forks in a similar manner as conventional CLs in AFM.

Figure 1 is a scanning electron microscope (SEM) image of a  $q$ Plus-sensor (QPS): one prong of a tuning fork is bonded to a mount, the other prong has a tip attached to it. The quality of the bond between the mount and the fixed prong is crucial for obtaining a high  $Q$  value. Using epoxy resins with fillers,  $Q$  values up to a few thousand in ambient

pressure can be achieved—about ten times higher than the  $Q$  of conventional CLs. The tuning forks used here have  $f_0^{\text{bare}} = 32\,768\text{ Hz}$  ( $=2^{15}\text{ Hz}$ ), the length of one prong is  $L = 3.0\text{ mm}$ , thickness  $t = 330\ \mu\text{m}$  and width  $w = 120\ \mu\text{m}$ . With the Young's modulus of quartz  $E = 7.87 \cdot 10^{11}\text{ N/m}^2$  and mass density<sup>11</sup>  $\rho = 2650\text{ kg/m}^3$  the theoretical spring constant is  $k = 0.25Ew(t/L)^3 = 3143\text{ N/m}$  and the theoretical eigenfrequency equals<sup>12</sup>  $f_0^{\text{bare}} = 1.015\sqrt{E/\rho w/(2\pi L^2)} = 32\,280\text{ Hz}$ —in good agreement with the nominal eigenfrequency. When the prongs are deflected by  $q'$ , the piezoelectric effect causes a voltage  $V$  across the electrodes. The sensitivity  $S$  of the forks of the type listed above was experimentally determined to  $S = V/q' = 6.6\ \mu\text{V/nm}$ .

The tip attached to the free prong is etched out of tungsten wire with an initial diameter of 0.25 mm by ac etching in 1 M KOH. The final diameter is approximately 0.15 mm and the length 1 mm. The eigenfrequency with attached tips drops to  $f_0 \approx 12\text{--}16\text{ kHz}$ . The apex of the tips as determined by scanning electron microscopy is approximately spherical with a radius of  $R_{\text{tip}} \approx 150\text{ nm}$ .

The QPS is operated in the frequency modulation mode as introduced by Albrecht *et al.*<sup>13</sup> Figure 2 is a schematic of the detection electronics. The QPS is placed on an actuator, the deflection signal is routed through a preamplifier, a phase

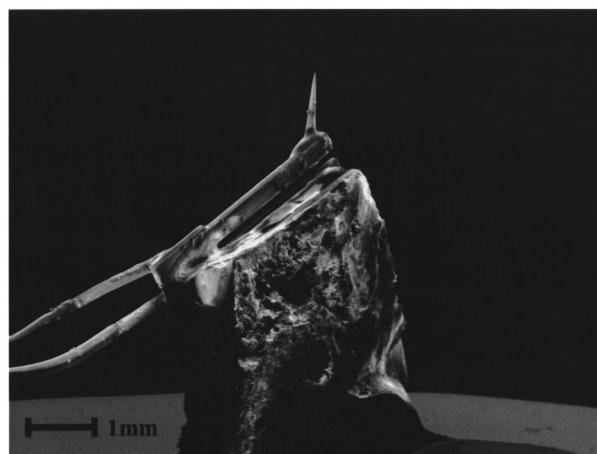


FIG. 1. Scanning electron microscope image of the force sensor.

<sup>a)</sup>Electronic mail: franz@giessibl@physik.uni-augsburg.de

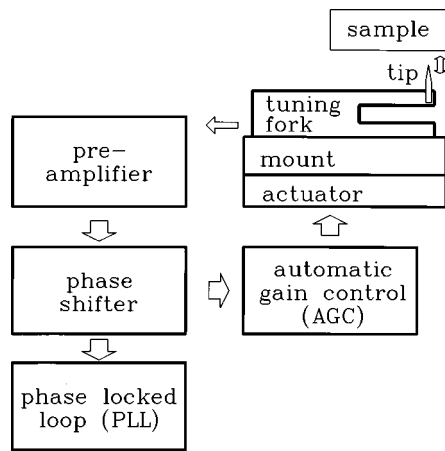


FIG. 2. Schematic of an atomic force microscope based on frequency modulation detection.

shifter and an automatic gain control circuit (AGC) before it is fed back to the actuator. The AGC adjusts for a constant vibration amplitude  $A_0$ . The deflection signal is also fed into a phase-locked-loop circuit (PLL) which converts the oscillation frequency  $f$  to a dc signal which is proportional to the difference between  $f$  and an adjustable setpoint. Forces  $F_{ts}$  between the tungsten tip and a sample cause the frequency to change from  $f_0$  to  $f = f_0 + \Delta f$ . The frequency shift can be calculated with first order perturbation theory:<sup>14</sup>

$$\Delta f(d) = -\frac{f_0^2}{kA_0} \int_0^{1/f_0} F_{ts}(d + A_0[1 + \cos(2\pi f_0 t)]) \times \cos(2\pi f_0 t) dt. \quad (1)$$

In principle,  $F_{ts}$  is attractive as long as  $d$ , the minimal distance between the front atom of the tip and the sample is positive. In vacuum, it is even possible to obtain atomic resolution by probing the attractive forces.<sup>15</sup> However, attractive forces are not very well reproducible in ambient conditions, it is much easier to work with the repulsive forces which arise upon contact. For a spherical tip and a flat sample, the repulsive forces are given by<sup>12</sup>

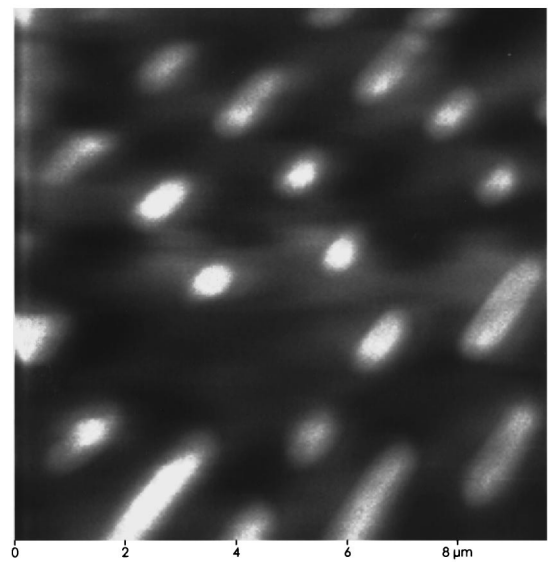


FIG. 4. Image of the metal foil from a compact disk. Scanning speed 12 lines per second (lps), tungsten tip,  $k = 3300$  N/m,  $A_0 = 150$  nm,  $\Delta f = 3$  Hz,  $f_0 = 13535$  Hz.

$$F_{ts}(d) = \frac{4}{3} E^* \sqrt{R_{tip}} (-d)^{1.5} \quad \text{for } d < 0 \quad (2)$$

and  $F_{ts} = 0$  for  $d > 0$  (Hertzian contact).  $E^*$  is the effective Youngs modulus given by<sup>12</sup>

$$\frac{1}{E^*} = \frac{1 - \mu_{sample}^2}{E_{sample}} + \frac{1 - \mu_{tip}^2}{E_{tip}}. \quad (3)$$

Evaluation of Eq. (1) for this force yields (for  $A_0 \gg -d$ ):

$$\Delta f(d) = \frac{f_0}{kA_0^{3/2}} \frac{2\sqrt{2}}{3\pi} E^* \sqrt{R_{tip}} d^2 \quad \text{for } d < 0 \quad (4)$$

and  $\Delta f = 0$  for  $d > 0$ . For comparing the data with results with other amplitudes and spring constants, a normalized frequency shift<sup>14</sup> is used:

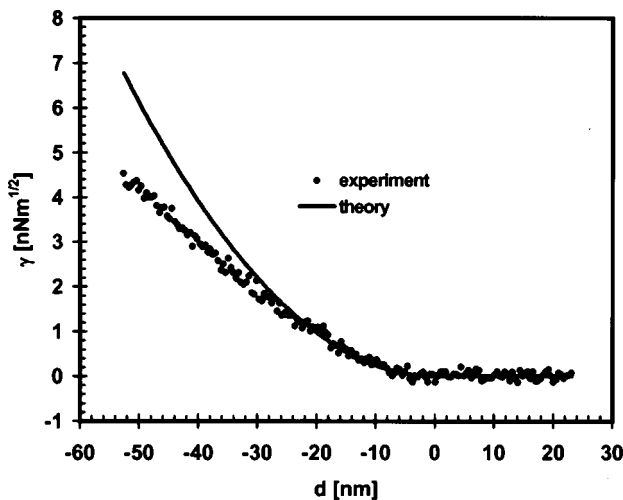


FIG. 3. Experimental and theoretical normalized frequency shift  $\gamma$  [ $= (\Delta f/f_0)kA_0^{3/2}$ ] versus distance for an aluminum sample and a spherical tungsten tip with a radius of 150 nm.

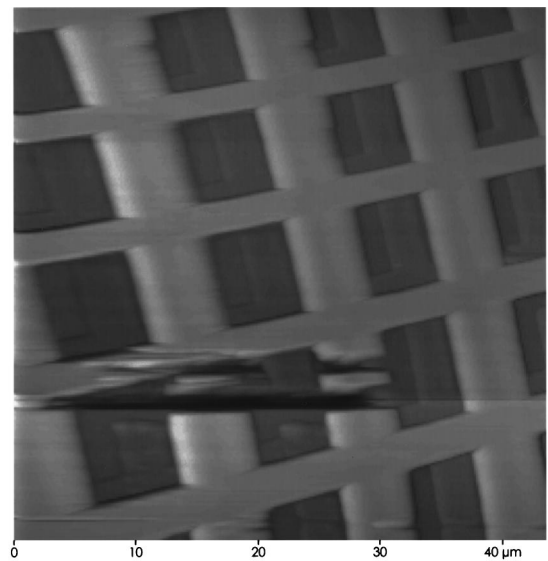


FIG. 5. Image of a test grating with 10  $\mu\text{m}$  pitch and 100 nm height, scanning speed 0.7 lps, sapphire tip,  $k = 3300$  N/m,  $A_0 = 250$  nm,  $\Delta f = 15$  Hz,  $f_0 = 27\,214$  Hz.

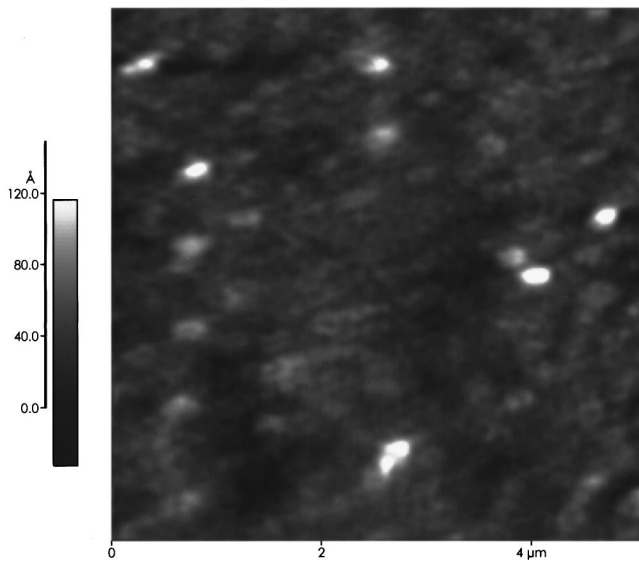


FIG. 6. Image of a processed silicon wafer, scanning speed 1 lps, tungsten tip,  $k=3300$  N/m,  $A_0=150$  nm,  $\Delta f=8$  Hz,  $f_0=13\,535$  Hz. The height of the white dots is  $\sim 8$  nm, their width  $\approx 100$  nm.

$$\gamma = \frac{\Delta f}{f_0} k A_0^{3/2}. \quad (5)$$

Figure 3 shows experimental and theoretical data for the normalized frequency shifts for a tungsten tip and aluminum surface. The parameters used were  $A_0=450$  nm,  $f_0=16\,083$  Hz,  $k=3300$  N/m and  $R_{\text{tip}}=150$  nm. For tungsten and aluminum, the effective Young's modulus is  $E^*=6.7 \times 10^9$  N/m<sup>2</sup>. For indentations  $d \lesssim 30$  nm, the experimental frequency shift reflects the quadratic behavior of Eq. (4). For larger indentations, the conditions for which the theoretical frequency shift was calculated (constant amplitude) are no longer fulfilled. Additional damping is noticeable for indentations  $d \gtrsim 30$  nm—the amplitude drops and the experimental frequency shift increases approximately linear with indentation. While this deviation is caused by strong interaction, the linear relationship between frequency shift and distance allows very fast and reliable operation of the microscope.

Figure 4 shows an image of a metal foil which was peeled off a compact disk. The image was obtained for a constant frequency shift  $\Delta f=3$  Hz with  $A_0=150$  nm. The normalized frequency shift is  $\gamma=35.8$  pN $\sqrt{\text{m}}$ —about 1000 times larger in magnitude than the normalized frequency shift in noncontact AFM with true atomic resolution.<sup>16</sup> The acquisition speed was 12 lines per second (lps) and the width of the image is  $9.6 \mu\text{m}$ , thus the scanning speed is  $230 \mu\text{m/s}$ —100 times faster than in previous implementations.<sup>9</sup> Figure 5 presents an image of a calibration grating. Here, the tip of the QPS is a small crystal of sapphire (approx. 0.3 mm diameter). The mass of this crystal is much less than the

mass of a tungsten tip, therefore the eigenfrequency of the fork dropped much less. However, the “ghosts” in the depressions of Fig. 5 indicate a double tip. Figure 6 is a  $5 \times 5 \mu\text{m}^2$  image of a processed silicon wafer. The white dots in the image are approximately 8 nm high and 100 nm wide. The vertical noise in the image is below 1 nm.

So far, this sensor has only been operated in ambient conditions with strong repulsive forces. The lateral resolution which has been demonstrated is in the order of 100 nm. Better resolution is expected when the sensor is operated in vacuum. A recent analysis<sup>17</sup> has shown that vertical resolution of a few pm should also be possible with rather stiff cantilevers with  $k \approx 1000$  N/m. Also, atomic resolution on Si (111)-(7 $\times$ 7) with an AFM with etched tungsten tips has been demonstrated recently.<sup>18</sup> Therefore, even atomic resolution might be achievable with this new type of force sensor. Compared to conventional CLs, the main advantages of this new sensor is its self sensing capability, i.e., no optics is required for sensing the deflection and its very low power dissipation in the order of nW, i.e., six orders of magnitude lower than with piezoresistive or optical detection methods.

The author wishes to thank Jochen Mannhart for discussions and Klaus Wiedenmann for taking the SEM image of the force sensor (Fig. 1). This work was partially supported by BMBF Grant No. 13N6918/1.

- <sup>1</sup>G. Binnig, C. F. Quate, and Ch. Gerber, *Phys. Rev. Lett.* **56**, 930 (1986).
- <sup>2</sup>J. B. P. Williamson, *Proc. Inst. Mech. Eng.* **182**, 21 (1967).
- <sup>3</sup>D. Sarid, *Scanning Force Microscopy* (Oxford University Press, New York, 1994).
- <sup>4</sup>M. Tortonese, R. C. Barrett, and C. F. Quate, *Appl. Phys. Lett.* **62**, 834 (1993).
- <sup>5</sup>T. Itoh and T. Suga, *Nanotechnology* **4**, 218 (1993).
- <sup>6</sup>F. L. Walls, in *Precision Frequency Control*, edited by E. A. Gerber and A. Ballato (Academic, Orlando, 1985), p. 276.
- <sup>7</sup>P. Guethner, U. Fischer, and K. Dransfeld, *Appl. Phys. B: Photophys. Laser Chem.* **B48**, 89 (1989); P. Guethner, Dissertation, University Konstanz, Germany, 1992.
- <sup>8</sup>K. Karrai and R. D. Grober, *Appl. Phys. Lett.* **66**, 1842 (1995).
- <sup>9</sup>H. Edwards, L. Taylor, W. Duncan, and A. Melmed, *J. Appl. Phys.* **82**, 980 (1997).
- <sup>10</sup>F. J. Giessibl, “qPlus Sensor”—Offenlegungsschrift DE196 33 546 A1, German Patent Office (1998).
- <sup>11</sup>H. Kuchling, *Taschenbuch der Physik* (Harri Deutsch, Thun and Frankfurt/Main, 1982).
- <sup>12</sup>C. J. Chen, *Introduction to Scanning Tunneling Microscopy* (Oxford University Press, New York, 1993).
- <sup>13</sup>T. R. Albrecht, P. Grütter, D. Horne, and D. Rugar, *J. Appl. Phys.* **69**, 668 (1991).
- <sup>14</sup>F. J. Giessibl, *Phys. Rev. B* **56**, 16010 (1997).
- <sup>15</sup>F. J. Giessibl, *Science* **267**, 68 (1995); S. Kitamura, M. Iwatsuki, *Jpn. J. Appl. Phys., Part 2* **34**, L145 (1995).
- <sup>16</sup>When imaging with true atomic resolution,  $\gamma \approx -30$  fN $\sqrt{\text{m}}$  is a typical value, see Table 1 in Ref. 17.
- <sup>17</sup>F. J. Giessibl, H. Bielefeldt, S. Hembacher, and J. Mannhart, *Appl. Surf. Sci.* (to be published).
- <sup>18</sup>R. Erlandsson, L. Olsson, and P. Martensson, *Phys. Rev. B* **54**, R8309 (1996).